Heliyon 10 (2024) e35589

Contents lists available at ScienceDirect

Heliyon

journal homepage: www.cell.com/heliyon

Research article

Role and mechanism of IRF9 in promoting the progression of rheumatoid arthritis by regulating macrophage polarization via PSMA5

Yue Guan [a], Xin Li [a], Hemin Yang [b], Siyu Xu [c], Lidong Shi [a], Yangyang Liu [a], Lingdan Kong [a], Ying Qin [a,*]

[a] Department of Rheumatology and Immunology, The Third Affiliated Hospital of Qiqihar Medical University, Qiqihar, China
[b] Central Laboratory, The Third Affiliated Hospital of Qiqihar Medical University, Qiqihar, China
[c] Inspection Center, The Third Affiliated Hospital of Qiqihar Medical University, Qiqihar, China

ARTICLE INFO

Keywords:
Rheumatoid arthritis
IRF9
PSMA5
Macrophage

ABSTRACT

Aim: To explore the mechanisms of IRF9 in the progression of rheumatoid arthritis(RA), and the effects of IRF9 on M1/M2 polarization.
Methods: RA dataset (GSE55457) was downloaded from GEO. Correlation analysis between IRF9 and its downstream target protein PSMA5 was performed using bioinformatics analysis. The M1/M2 cell ratio of peripheral blood mononuclear cells which from 20 healthy specimen and 40 RA patients was determined. The expression of IRF9 and PSMA5 was detected using qPCR and Western blot. Then, knockdown IRF9 in RAW264.7 cell line (sh-IRF9 RAW264.7) was constructed. The effect of sh-IRF9 RAW264.7 on RA was explored by constructing a CIA mouse model.
Results: IRF9 is upregulated in RA and is of good early screening effect. The results of pathway analysis showed that IRF9 targets and regulates the PSMA5 signaling pathway. IRF9 and PSMA5 were significantly elevated in RA patients, M1/M2 ratio was also increased. The effects of IRF9 on RAW264.7 macrophages were deeply explored in vitro, revealing that knockdown of IRF9 suppressed PSMA5, M1/M2 ratio and the secretion of pro-inflammatory factor in RAW264.7. In mouse in vivo experiments, sh-IRF9 RAW264.7 cells were found to modulate RA by down-regulating PSMA5, modulating the M1/M2 ratio through enhancing the anti-inflammatory factor, and suppressing the pro-inflammatory factor.
Conclusion: IRF9 promoted the progression of RA via regulating macrophage polarization through PSMA5.

1. Introduction

Rheumatoid arthritis (RA) is a long-term and advancing inflammatory condition distinguished by continuous inflammation of the synovial membrane, resulting in symmetrical polyarthritis affecting both small and large joints. This condition can lead to joint and periarticular structure damage, as well as systemic inflammation [1,2]. The global occurrence of RA ranges from 0.5 % to 1 %, with

* Corresponding author. Department of rheumatology and immunology, the Third Affiliated Hospital of Qiqihar Medical University, No.27, Taishun Street, Tiefeng District, Qiqihar 161000, China.
E-mail address: Qy15603629068@qmu.edu.cn (Y. Qin).

https://doi.org/10.1016/j.heliyon.2024.e35589
Received 2 April 2024; Received in revised form 31 July 2024; Accepted 31 July 2024
Available online 5 August 2024

women exhibiting a prevalence more than twice as high as that in men [3]. Although the variety of drugs available for the treatment of RA has gradually increased with the development of biotechnology, there are still a large number of patients who do not receive standardized treatment due to various reasons. Therefore, it is imperative to create novel therapeutic medications that are tailored towards treating RA.

The gene chip technology possesses the advantages of high throughput, seamless integration, and rapidity, among others. It finds extensive applications in medicine and various other domains, enabling the exploration of disease molecular mechanisms at the genetic level [4]. The aim of this research is to ascertain the key genes regulating macrophages in RA patients by integrating gene chip data and analyzing the dataset using bioinformatics methods. The objective of this analysis is to improve the comprehension of the roles and routes linked with these pivotal genes, predict their roles in RA, and provide novel insights into the inflammatory mechanism underlying this disease.

Monocytes, which come after neutrophils, serve as the second line of defense cells within the innate immune system. They exhibit phenotypic and functional heterogeneity as well as plasticity, enabling their differentiation into macrophages [5]. The inflammatory response serves as the central link in the pathogenesis of RA, with macrophages playing a pivotal role in promoting synovial tissue inflammation among RA patients. These macrophages are abundantly present within cartilage tissues and synovial cells, tightly intertwined with the inflammatory processes associated with RA [6–8]. Studies have demonstrated that macrophages accumulate and polarize within the joint cavity and synovium during the progression of RA, with activated M1-type macrophages secreting a plethora of cytokines implicated in RA [9]. Nevertheless, the precise mechanism underlying the role of macrophages in RA pathogenesis remains elusive and warrants further investigation.

Under the influence of the same subtle environmental factors both in vivo and in vitro, macrophages can differentiate into two distinct subpopulations: M1-type macrophages and M2-type macrophages. As a common marker for M1 macrophages, the expression of iNOS can lead to the secretion of numerous pro-inflammatory cytokines (such as TNF-α, IL-1β, and IL-6), which activate fibroblasts and osteoclasts. This subsequently accelerates inflammatory reactions within the body, ultimately resulting in joint destruction [10]. M2 macrophages, whose common markers include CD206, promote angiogenesis, tissue remodeling and repair by producing anti-inflammatory cytokines (such as TGF-β, IL-10) in large quantities [11]. The presence of a substantial number of activated macrophages in the synovium is an early hallmark of RA. When certain elements contribute to an elevation in the percentage of M1 macrophages or a reduction in the percentage of M2 macrophages, it results in an inequilibrium within the M1/M2 ratio, which signifies the advancement of RA. Therefore, it is crucial to investigate the molecular mechanisms that influence the M1/M2 balance for regulating RA progression.

The interferon regulatory factor (IRF) family is currently present in a total of nine mammalian species (IRF1∼9), primarily exerting transcriptional control over the immune system and cell growth. The initial identification of IRFs was attributed to their role in activating the expression of type I interferon genes, with IRF1, IRF3, IRF5, IRF7 and IRF9 all possessing this function [12]. Notably, among these factors, both IRF3 and IRF7 exhibit the most pronounced effects. The Type I interferon exerts a potent antiviral function by activating the JAK-STATs pathway and inducing the expression of an extensive array of antiviral-related proteins. When the body is infected by viruses and other pathogenic microorganisms, the PRR-mediated signaling pathway not only activates NF-κB but also phosphorylates and activates IRF3, IRF5, and IRF7, thereby inducing the expression of type I interferon and other pro-inflammatory cytokines in the nucleus. In addition to their functions in differentiated immune cells, certain IRFs (IRF1, IRF2, IRF4, and IRF8) play crucial roles in undifferentiated immune cells including DC cells, NK cells, myeloid cells, B cells, and T cells. Upon activation, these IRFs facilitate the maturation and differentiation of pertinent immune cells, thereby triggering the initiation of the acquired immune response [13].

The primary role of IRF9, unlike other IRFs, is to facilitate the formation of the protein complex ISGF3 alongside phosphorylated STAT1 and STAT2, thereby actively participating in the JAK-STATs pathway. IRF9 is an essential transcription factor mediating the antiviral response to type I interferon [14], and it is an essential transcription factor mediating the type I scrambler antiviral response, and is part of the purified protein subunit of the ISGF3 complex, which regulates interferon-stimulated genes. IRF9 is involved in the control of cellular growth, development of tumors, cardiovascular disorders, inflammatory responses, and various other biological mechanisms [15]. In recent years, many studies have reported that IRF9 is significent in the pathogenesis and progression of several autoimmune diseases, including RA [16] and systemic lupus erythematosus (SLE) [17]. It was found that IRF9 was significantly elevated in $CD14^{+}$ monocytes of RA patients and positively correlated with disease activity indicators such as 28 joint disease activity (DAS28), erythrocyte sedimentation rate (ESR) and C-reactive protein (CRP), revealing that IRF9 is crucial in the pathophysiological process of RA [17]. But is it involved in regulating macrophage polarization in RA disease? What is its critical mechanism for guiding macrophage polarization? It remains to be further explored.

In summary, there are fewer studies on the role played by IRF9 in the pathogenesis of RA, and there has not been any study on IRF9 in RA through its involvement in the regulation of macrophage program. Therefore, the objective of this research is to delve deeper into the function of IRF9 in controlling macrophage polarization and its impact on both RA pathogenesis and systemic damage. This will be achieved by examining the differential expression of IRF9 and its downstream target genes and proteins, as well as analyzing their correlation with clinical and laboratory indexes of patients. These discoveries will improve our comprehension of the development of RA and assist in choosing suitable treatment plans.

2. Methods

2.1. Reagents

Incomplete Freund's adjuvant (7002), complete Freund's adjuvant (7001), bovine type II collagen (20022) were purchased from Chondrex, USA. Penicillin-streptomycin double antibody as well as fetal bovine serum was purchased from Gibco, USA. Human peripheral blood single nucleated cell isolate was purchased from Solarbio, China. IRF9 (GTX62933) antibody, PSMA5 (GTX63385) antibody were purchased from GeneTex, USA, CD68 (ab303565) antibody, CD206 (ab64693) antibody, iNOS (ab178945) antibody, β-tubulin (ab7291) antibody antibody were purchased from abcam, USA. Human IL-10 ELISA kit (ml064299), mouse IL-10 ELISA kit (mIC50274-1), human TGF-β ELISA kit (ml064258), mouse TGF-β ELISA kit (ml057830), human IL-1β ELISA Kit (ml058059), mouse IL-1β ELISA Kit (ml098416), mouse TNF-α ELISA Kit (mIC50536-1), and human TNF-α ELISA Kit (ml077385) were purchased from Shanghai Enzyme-Link Bio-Tech. Ltd.

2.2. Data collection and analysis

Relevant histologic data were collected through the GEO database. In the GSE55457 gene expression matrix, $P < 0.001$ was taken for differential expression analysis to obtain differentially expressed genes, and the screening of differentially expressed genes was based on $|\log2(\text{Fold Change})| > 1$, $P < 0.001$. The differential analysis was carried out using the R software Limma package. The ROC curve was plotted with the true positive rate (sensitivity) as the vertical coordinate and the false positive rate (1-specificity) as the horizontal coordinate. The size of the area under the curve (AUC) was evaluated. Correlation analysis was performed using cibersort analysis.

2.3. Target gene prediction

FIMO (https://meme-suite.org/meme/tools/fimo) provides output in a variety of formats, including HTML, XML, and several Santa Cruz Genome Browser formats. The program is very efficient, allowing DNA sequences to be scanned at a rate of 3.5 Mb/s on a single CPU. Flanking region sequences (upper 2000 bp) for each gene in the entire network were extracted from the Integrated BioMart database (http://asia.ensembl.org/biomart/martview). To identify locally over-represented IRF9 binding sites, the FIMO tool, which detects IRF9 target genes, was used.

2.4. Samples collection

This research recruited a cohort of 40 RA patients and obtained 20 whole blood samples from healthy individuals who underwent medical checkups at our hospital for this study. All serum samples were obtained from the Third Affiliated Hospital of Qiqihar Medical University. All sampled patients signed informed consent and met the ethical standards of the Ethics Committee of The Third Affiliated Hospital of Qiqihar Medical University (NO. 2023LL-69) and with the 1964 Helsinki declaration and its later amendments or comparable ethical standards.

2.5. Isolation of human peripheral blood mononuclear cells(PBMC)

Peripheral blood single nucleated cells (PBMC) were isolated from peripheral blood using Ficoll density gradient centrifugation. PBMC were suspended at the interface of the plasma and the stratified fluid, forming a whitish membranous layer of material, and isolated PBMC could be obtained by aspirating this layer of cells and washing and resuspending them in a culture medium.

2.6. Cell lines

THP-1 cell lines as well as RAW264.7 cell lines were from the American Type Culture Collection(ATCC) and cultured in high-sugar DMEM (10 % fetal bovine serum, 1 % dual antibody) complete medium with 5 % CO_2 at 37 °C.

2.7. Animals

The SPF-grade 8-week-old DBA/1 male mice (18 ± 2 g) were procured from Beijing Viton Lihua Laboratory Animal Technology Co Ltd (Beijing, 2016-0006), and housed in the SPF-grade animal facility of the Laboratory Animal Center. The animals were kept in a controlled environment, with the temperature maintained at approximately 22 °C and humidity levels ranging from 40 % to 60 %. They were provided with a standard diet and access to water freely. The light-dark cycle was set at a duration of 12 h each. Random allocation into four groups was performed, with each group consisting of ten animals. The groups were presented as follows: normal group, CIA group, LPS group(LPS-treated RAW264.7 cell), and sh-IRF9 group(the sh-IRF9 RAW264.7 cell). The mice were successfully modeled after 7 days of strengthened immunization, and the intervention was started. The animal experiment was approved by the Animal Ethical Care Committee of the Third Affiliate Hospital of Qiqihar Medical University (NO.AECC- 2023-003).

2.8. Establishment of CIA animal model

The Bovine type II collagen solution, with a concentration of 2 mg/mL, was combined with an equal volume of Fuchs' complete adjuvant (CFA) at the same concentration and chilled on ice. Subsequently, it was transformed into a water-in-oil state using a high-speed homogenizer. The above mixture (100 μL) was subcutaneously injected into the tail root of each mouse, and Fuchs' incomplete adjuvant (IFA) was administered as a replacement for CFA after 21 days. The remaining steps of the procedure were identical to those of the initial immunization, and the second booster immunization was conducted. In the sh-IRF9 group, IRF9 shRNA (2 mg/kg) was injected intravenously into the tail vein on the 24th day after the initial immunization, and equal amounts of saline were injected into the Model and Normal groups. Skin color, skin temperature, skin infection status, hindfoot action, and knee joint swelling status were observed continuously in the hindfoot and knee joints of rats in each group.

Joint index scoring: The hind feet of rats were observed continuously, and the joint symptom scores were assessed using the arthritis index score method. Two hind feet of rats were quantitatively scored based on the extent, and deformity of redness and swelling of the joints, loss of shiny and dry hair, and reduced activity. Subsequently, the average arthritis scores for each group of rats were determined using the joint symptom scores of individual rats. The scoring criteria for joint symptoms were as follows: arthritis was divided into 5 grades: 4 for deformation of the joint and inability to bear weight, 3 for severe swelling, 2 for moderate swelling of the joint, 1 for red spots or mild swelling, and 0 for no redness or swelling. The total number of points for arthritis is 16.

2.9. qPCR

The extraction of total RNA was performed utilizing the Trizol reagent(R0016, Beyotime Biotechnology, China). The RNA was transcribed in reverse to generate cDNA. Real-time qPCR analysis was carried out. The relative expression levels were determined by $2-(^{\Delta\Delta}Ct)$. The mean threshold period (Ct) value for each transcript was normalized to β-actin(A5092, Bimake, China). Primer sequences was in Table 1.

2.10. Construction of IRF9-shRNAs

The shRNA was designed and synthesized on clontech's website, the primers were diluted to 100 μM, and the forward and reverse primers of the single-stranded shRNA were turned into double-stranded, PCR was performed. The vector PSIREN (*Bam*HI and *Eco*RI) was enzymatically digested, and the fragment was ligated to the digested vector, transformed, and plasmid construction was performed(Table 2).

2.11. Chromatin immunoprecipitation (ChIP)

The cells were subjected to formaldehyde treatment, followed by cell collection for sonication and fragmentation. Antibodies targeting specific proteins were then added, which not only bound to the target protein-DNA complexes but also interacted with each other. Protein A was subsequently introduced to bind with the antibody-target protein-DNA complexes, leading to precipitation. The precipitated complexes were subjected to washing in order to eliminate any non-specific binding, followed by elution. This process resulted in the enrichment of target protein-DNA complexes. Subsequently, de-crosslinking and purification steps were performed on the enriched DNA fragments for PCR analysis.

2.12. Western-blot

Total protein was extracted from cells. Protein concentration was quantified according to the bicinchoninic acid (BCA) assay. SDS-PAGE electrophoresis was performed. The proteins that were separated underwent transfer onto a PVDF membrane(ISEQ00010, Millipore, USA) utilizing a transfer device. The PVDF membrane was incubated for 1 h with 5 % skimmed milk, followed by washing with TBS. The primary antibody(Cell Signaling Technology, USA) of ferroptosis marker protein was incubated at 4 °C overnight. Afterwards, the secondary antibody was introduced and allowed to incubate for a duration of 1 h. Finally, the PVDF membrane was exposed for detection using a chemiluminescent imaging system.

2.13. ELISA

Dispense 50 μL of diluted standard and 50 μL of the sample to be tested into the reaction wells, promptly add 50 μL of biotin-labeled antibody. The template should be covered, gently shaken and mixed, and then incubated at 37 °C for 1 h. Shake out the excess liquid

Table 1
Primer sequences.

Gene	Forward primer,5′-3′	Reverse primer,5′-3′
IRF9	CTGCTCACCTTCATCTACAACG	ACTAGGATGCCCCTCTCAA
PSMA5	TGCCATGTCTCGTCCCTTTG	TTTGTTGCATTCAGCTTCTCCT
GAPDH	TTGTCTCCTGCGACTTCAAC	GTCATACCAGGAAATGAGCTTG

Table 2
Primer sequences.

Gene	Forward primer,5′-3′	Reverse primer,5′-3′
sh-IRF9	GATCCGGATAACATACCTGCCTTCTTCAAGAGAGAAGGCAGGTATGTTATCCTTTTTTG	AATTCAAAAAAGGATAACATACCTGCCTTCTCTCTTGAAGAAGGCAGGTATGTTATCCG

from the wells, fill each well with washing solution, agitate for 30 s, discard the detergent by shaking off, gently dry with absorbent paper, repeat this process three times. Add 80 μL of streptavidin-HRP conjugate to each well, gently agitate and mix, incubate at 37 °C for 30 min; remove the liquid from the wells by shaking off, and perform three washes; add 50 μL of substrate A and B to each well, gently agitate and mix, and incubate at 37 °C for 10 min while avoiding exposure to light. Reposition the plate, swiftly introduce 50 μL of termination solution, and promptly assess the results subsequent to the addition of termination solution. Measure the optical density (OD) value at the designated wavelength for each well.

2.14. Statistic analysis

The data was subjected to statistical analysis using the GraphPad 9 software. The data are reported as the mean value with mean ± SEM. The statistical disparities between two groups were assessed using a *t*-test. Statistical differences between means of multiple groups were compared using analysis of variance (ANOVA). The statistical significance was determined by considering P-values less than 0.05.

3. Results

3.1. Analysis of RA dataset

In order to explore the mechanisms underlying the development of RA, the gene sequencing dataset of RA patients was analyzed. The data was obtained from the GEO database. The GSE55457 gene expression matrix was subjected to differential analysis using the R software Limma package, which revealed a statistically significant upregulation of IRF 9 in RA(Fig. 1A, Supplementary Figs. 1A–1B). The efficacy of IRF 9 in early screening for RA was assessed by constructing the ROC curve, which yielded a perfect ROC = 1, indicating the crucial role of IRF 9 in identifying RA at an early stage(Fig. 1B). What's more, IRF 9 was positively associated with M1/M2 (P =

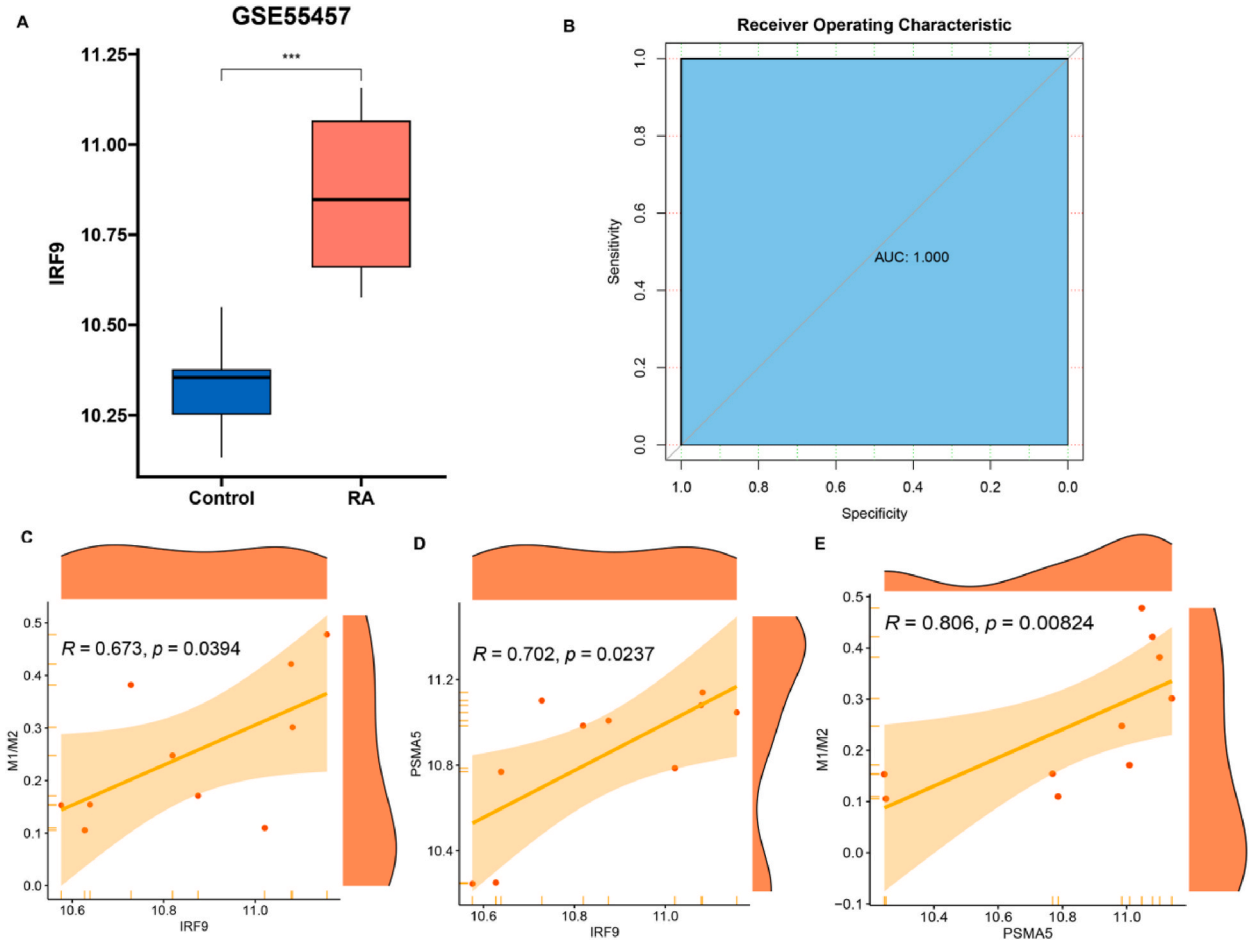

Fig. 1. Bioinformatic analysis of dataset GSE55457. A. Box plot of IRF9 expression in GSE55457. B. ROC plot of IRF9 and RA. C. Linear regression of IRF9 and M1/M2. D. Linear regression of IRF9 and PSMA5. E. Linear regression of PSMA5 and M1/M2, ***P < 0.001.

0.0394, R = 0.673) (Fig. 1C). The aforementioned findings suggested that IRF9 might exert a pivotal role in the pathogenesis or progression of RA through its involvement in the regulation of macrophage polarization.

In order to further investigate the regulatory role of IRF9 in macrophage polarization and its impact on downstream molecule expression, the correlation analysis between IRF9 and its target genes was conducted. The findings demonstrated a noteworthy association between PSMA5 and IRF9, indicating a positive correlation (P = 0.0237, R = 0.702) (Fig. 1D). Furthermore, there was a notable association between PSMA5 and M1/M2 ratio (R = 0.806, P = 0.00824) (Fig. 1E), suggesting that PSMA5 might be a critical downstream target of IRF9 for macrophage polarization.

3.2. IRF9 was significantly upregulated in PBMC of RA patients

The bioinformatics analysis revealed a significant correlation between the upregulation of the IRF9 gene and the onset of RA. To indicate the mechanism underlying the impact of the IRF9 on RA, this research recruited a cohort of 40 RA patients and obtained 20 whole blood samples from healthy individuals who underwent medical checkups at our hospital for this study. Using flow cytometry,

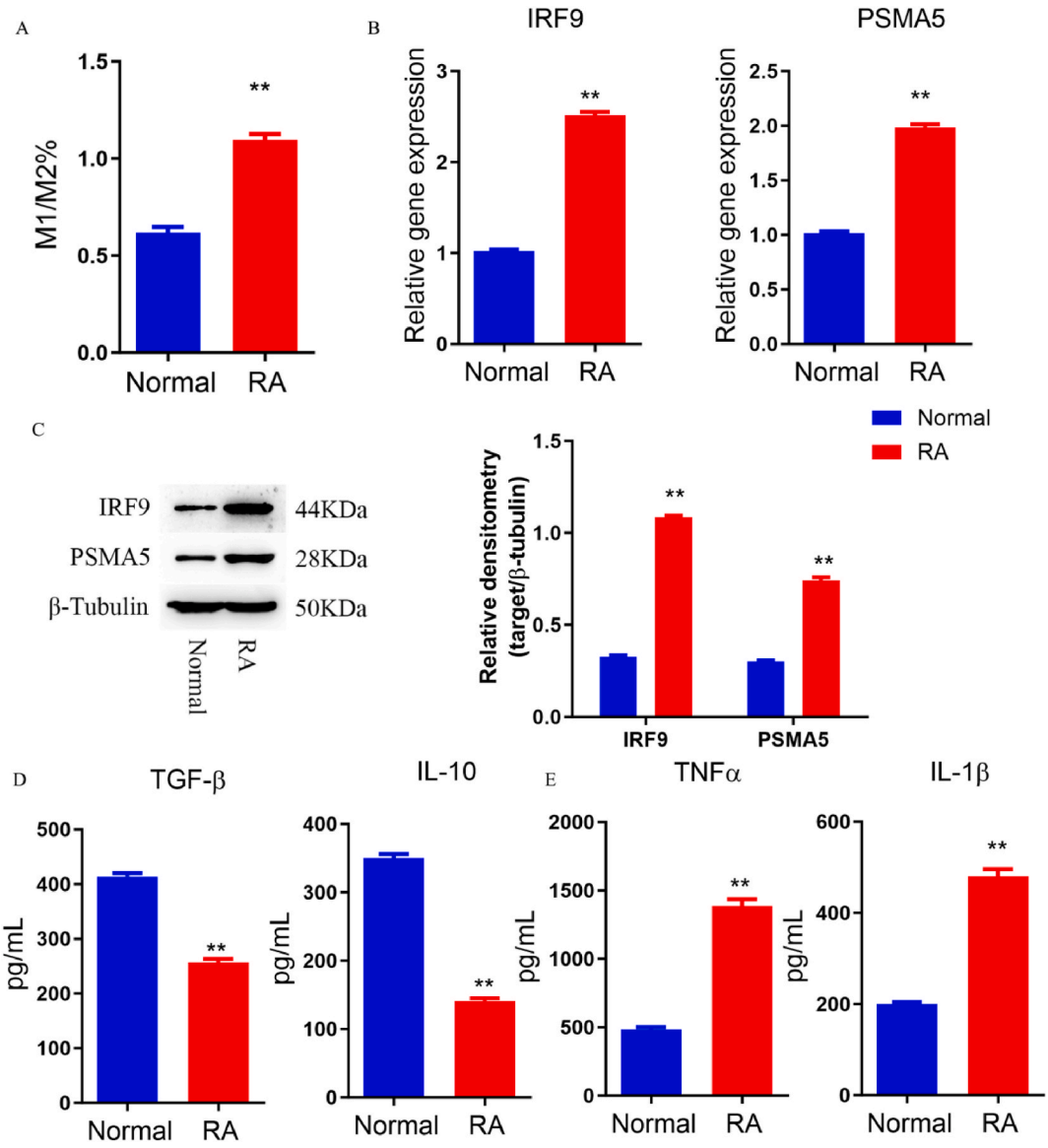

Fig. 2. IRF 9 was significantly upregulated in PBMC of RA patients
A. M1/M2 cell ratio in PBMC of RA patients. B. qPCR for the expression of IRF9 and PSMA5 in PBMC. C. Western blot for the protein expression level of IRF9 and PSMA5 in PBMC. D. ELISA for the expression of TGF-β and IL-10 in serum. E. ELISA for the expression of TNF-α, IL-1β in serum. Data were expressed as mean ± standard deviation (n = 6) *p < 0.05, **P < 0.01, ***P < 0.001, ****P < 0.0001.

we conducted an analysis on the polarization of macrophages in PBMC from both healthy individuals and RA patients. The findings indicated that PBMC from individuals with RA exhibited an elevated M1/M2 ratio in comparison to those without any health conditions(Fig. 2A). The mRNA as well as protein expression of IRF9 and PSMA5 was detected, the findings indicated that there was an increase in the levels of these markers among individuals with RA when compared to health cases(Fig. 2B and C, Supplementary Fig. 2). And the serum levels of TNF-α and IL-1β were increased, while TGF-β and IL-10 were decreased in RA patients (Fig. 2D and E).

3.3. IRF9 regulated PSMA5

Next, in vitro experiments were used to explore the mechanism underlying the regulation of RA by IRF9. To provide additional validation of IRF9's binding to the promoter region of PSMA5 in both human and mouse cells, ChIP assay was carried out. ChIP results revealed that IRF9 binds to the promoter of PSMA5 in both human and mouse cells (Fig. 3A and B).

Macrophages serve as the primary effector cells in immune response. To investigate whether IRF9 affects the progression of RA through regulation of macrophage polarization, an in vitro model was established using LPS-treated RAW264.7 cells to induce macrophage polarization. What's more, Western blot was used to identify the expression of CD68(total macrophage surface molecular markers) and iNOS(surface molecular marker of M1 macrophages), as well as CD206(surface molecular marker of M2 macrophages) (Fig. 4A–C, Supplementary Fig. 3). The results demonstrated that, in comparison to the LPS group, the sh-IRF9 group exhibited a significant decrease in iNOS expression, an increase in CD206 expression, and a reduction in the M1/M2 ratio. These findings suggest that IRF9 plays a crucial role in RAW264.7 cell activation and polarization function. The expression of PSMA5 exhibited a decline upon the knockdown of the IRF9(Fig. 4D). After knockdown of IRF9 in the LPS-induced RAW264.7 cell polarization model, the expression of TNF-α and IL-1β were reduced, whereas IL-10 and TGF-β were increased. In the RAW264.7 cell polarization model in which PSMA5 was knocked down, the induction of LPS did not result in a significant increase in the expression of IL-1β and TNF-α in the supernatants of RAW264.7 cells, thereby further confirming PSMA5 as a target molecule of IRF9 in the process of RA (Fig. 4E and F).

3.4. The role of IRF9 in CIA mice mechanism

After twenty-eight days from the initial immunization, the intervention of IRF9 shRNA was initiated. Simultaneously, weekly monitoring of bilateral metatarsophalangeal joint thickness in both the normal group and CIA mice commenced, along with clinical scoring. The results demonstrated a significant increase in metatarsophalangeal joint thickness in the CIA mice compared to those in the normal group ($P < 0.05$). The metatarsophalangeal joint thickness of CIA mice group was found to be the highest on day 35, and following the intervention of cell injection, a gradual decrease in joint thickness was observed. The most significant reduction occurred on day 49 ($P < 0.05$). By day 56, the metatarsophalangeal joint thickness of CIA mice in the sh-IRF9 group had significantly decreased to a level close to that of normal mice(Fig. 5A). The clinical scores of CIA mice group were significantly higher compared to those in the normal group (P less than 0.05). The highest clinical scores were observed in CIA mice on day 35, and following IRF9 shRNA intervention, there was a gradual decrease in the clinical scores of CIA mice. By day 56, the clinical scores of CIA mice in the sh-IRF9 group significantly decreased (P less than 0.05) and approached those of the normal group(Fig. 5B).

The expression of IRF9 and PSMA5 were examined in the synovial tissues of the ankle joints of the mice in each group. The results showed that the mRNA and protein of IRF9 as well as PSMA5 was elevated in the CIA model group compared with the normal control group, and was reduced in the sh-IRF9 group(Fig. 6A and B, Supplementary Fig. 4). To explore the effect of IRF9 on macrophage polarization in the synovial tissues of RA ankle joints in each group of mice, Western blot was performed. The results demonstrated that, in comparison to the normal group, the CIA group exhibited up-regulated CD68 and iNOS, along with a predominant distribution of M1 macrophages. However, upon replacement with sh-IRF9 RAW264.7 cells, there was a decrease in iNOS expression within mouse ankle synovial tissues compared to the CIA group. Additionally, there was a gradual increase in CD206 expression and a shift towards predominantly M2 type macrophage distribution(Fig. 6C–E, Supplementary Fig. 5). ELISA was used to analyze the effect of sh-IRF9 RAW264.7 on inflammation-related cytokines in serum. The findings indicated that when compared to the CIA group and the RAW264.7 group, the serum expression of TNF-α and IL-1β were decreased, while IL-10 and TGF-β were increased in the sh-IRF9 group (Fig. 6F and G).

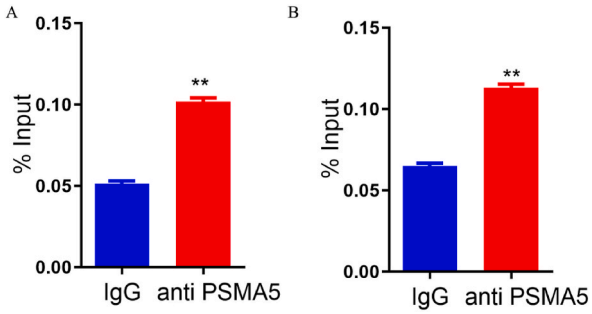

Fig. 3. ChIP assay to validate IRF9 binding in the PSMA5 promoter region in THP-1 cells (A) and RAW264.7 cells (B). **$P < 0.01$.

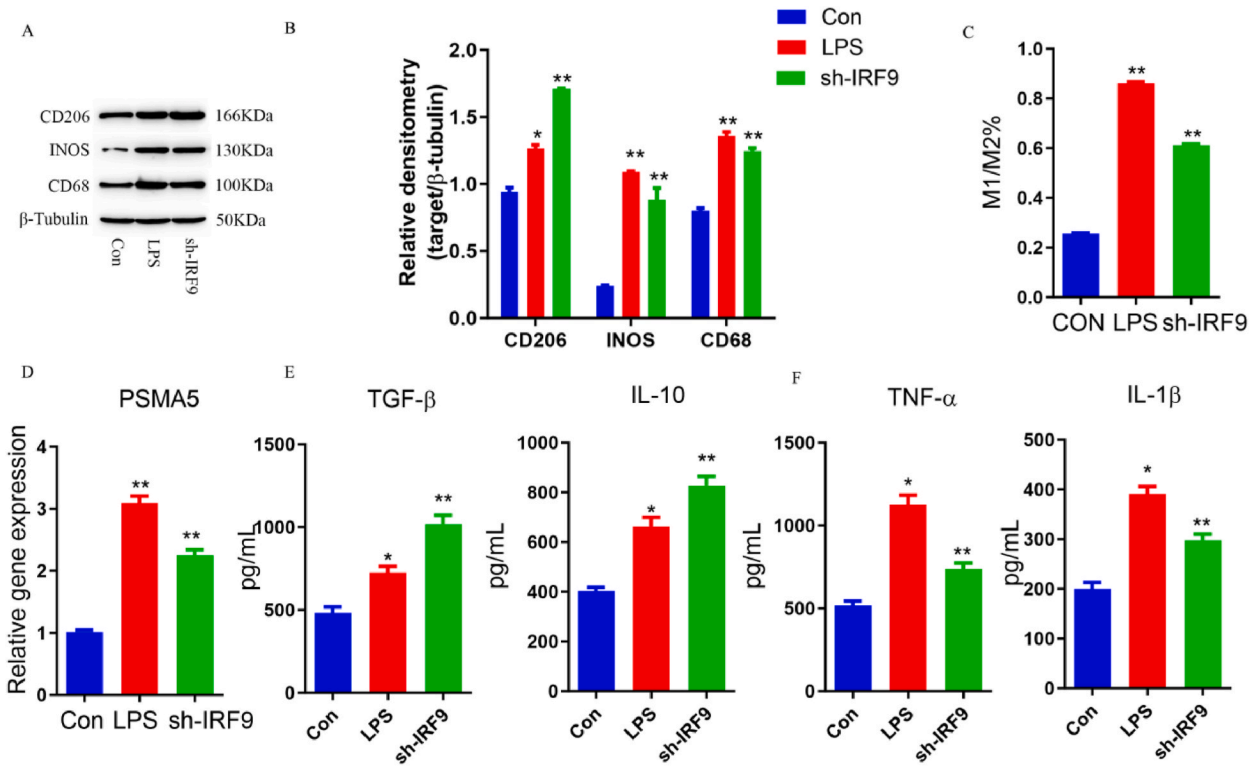

Fig. 4. IRF9 regulated macrophage M1/M2 polarization and conversion.
A-B. Western blot for expression of CD68, iNOS and CD206 in each group of cells. C. Proportion of M1 and M2 type macrophages. D. qPCR for PSMA5 expression in each group of cells. E. ELISA assay for expression of IL-10 and TGF-β in cell supernatants. F. ELISA assay for expression of IL-1β, TNF-α in cell supernatants. Data were expressed as mean ± standard deviation (n = 3), *p < 0.05, **P < 0.01.

4. Discussion

RA is a complex systemic disease with pathologic changes including synovitis, angiogenesis, and bone and cartilage degeneration [18]. The prior research has provided the crucial involvement of macrophages, as pivotal inflammatory effector cells, in the pathological progression of RA [19]. On the one hand, macrophage activation can be used as an early indicator for detecting RA, and on the other hand, macrophages are able to interact with other non-immune cells(osteoclasts) and immune cells through secretion, polarization and phagocytosis and thus influence the process of RA. The phagocytic capacity of macrophages has been a crucial indicator of their immunomodulatory function. This study specifically investigated the regulatory role of IRF9 in modulating macrophage function.

By conducting a comprehensive analysis of the RA GSE55457 datasets and integrating it with advanced bioinformatics techniques, we identified an up-regulation of IRF9 in RA, potentially implicating its involvement in macrophage polarization. However, the precise regulatory mechanism underlying this phenomenon remained elusive. The initial identification of IRF9 was as a constituent of the potent transcription factor interferon-stimulated gene factor 3, which is responsible for initiating the transcription of numerous interferon-stimulated genes to trigger an antiviral response. The role of IRF9 encompasses a diverse array of functions in pathogen isolation and disease amelioration. Remarkably, there is a paucity of comprehensive information regarding the multifaceted mechanisms underlying the functionality of IRF9, with the exception being its related to STAT1 as well as STAT2. More comprehensive investigations are warranted to elucidate the underlying mechanisms governing IRF9's modulation of transcriptional as well as translational activities. Specifically, further exploration is required to unravel the precise role of IRF9 in both promoting and attenuating inflammation. Although not explicitly discussed, the upregulation of IRF9 by the c-Myc proto-oncogene suggests its involvement in tumorigenesis [20]. Therefore, we hypothesized that aberrant macrophage metabolism in RA may be linked to the expression of IRF9. By conducting bioinformatics analysis, it was confirmed that PSMA5 exhibited a significant and positive correlation with both macrophage polarization and IRF9 levels in RA. Furthermore, online target gene prediction revealed that IRF9 directly binds to PSMA5. Based on this, researchers hypothesize that PSMA5 may serve as a crucial downstream molecule of IRF9, facilitating the regulation of macrophage polarization and ultimately contributing to the pathogenesis of RA. The PSMA5 protein, serving as the a5 subunit of the proteasome complex, plays a crucial role in mediating the ubiquitination-proteasome pathway [21]. As an ATP-dependent multisubunit protease, the proteasome plays a crucial role in protein degradation within eukaryotic cells. Specifically, it targets proteins for degradation through the ubiquitination-proteasome pathway and is involved in a wide range of essential biological processes across organisms [22–24]. The latest research findings indicate that PSMA5 exerts inhibitory effects on interferon-I (IFNI) production and facilitates T-cell-mediated immunosuppression [25,26]. However, the regulatory relationship between IRF9 and

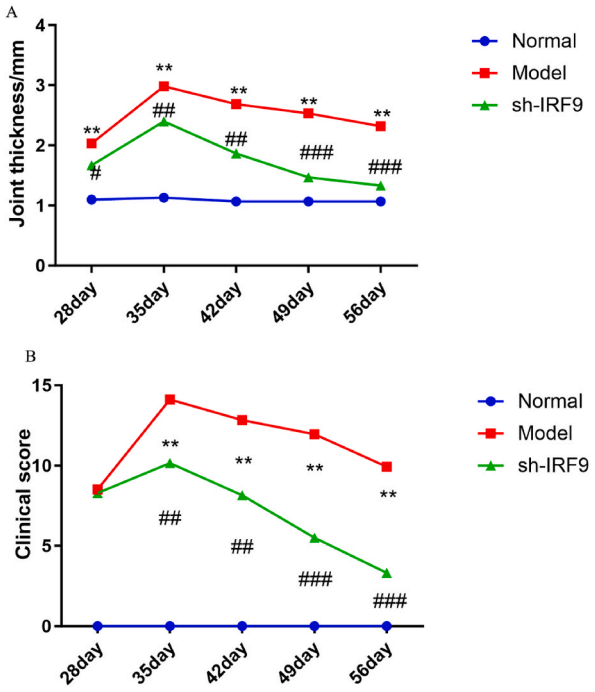

Fig. 5. Bilateral metatarsophalangeal joint thickness and Clinical scores
A. Metatarsophalangeal joint thickness measurements in CIA mice. B. Clinical scores in CIA mice. Compared with the normal group *P < 0.05, **P < 0.01, ***P < 0.001, ****P < 0.0001, compared with the model group #P < 0.05, ##P < 0.01, ###P < 0.001, ####P < 0.0001.

PSMA5-mediated macrophage polarization in RA progression has not been reported yet.

The present study aimed to investigate the regulatory role of IRF9 on macrophage function by specifically targeting and down-regulating IRF9 expression in macrophages. By silencing IRF9 in RAW264.7 cells, we observed alterations in the expression of PSMA5, the ratio of M1/M2-type macrophages, and the levels of their associated proteins, thereby reflecting the impact of IRF9 on macrophage polarization function. The knockdown of the IRF9 in RAW264.7 cells resulted in a down-regulation of PSMA5, subsequently impacting the immune response to RA. The impact of IRF9 on the secretory function of macrophages was evidenced by alterations in IL-10, TGF-β, IL-1β, and TNF-α. Notably, IL-10 exerted inhibitory effected on the release of inflammatory mediators from macrophages. TGF-β governed anti-inflammatory and immunosuppressive responses while playing a pivotal role in self-tolerance(Fig. 7). IL-1β primarily contributed to RA through its induction of osteoclastogenesis, resulting in cartilage and bone destruction. TNF-α caused synovial hyperplasia and cartilage erosion [21,27–29]. The present study investigated the expression of iNOS and CD206 in LPS-treated RAW264.7 cells with sh-IRF9. The findings demonstrated a significant reduction in the M1/M2 ratio, decreased levels of iNOS, increased levels of CD206, elevated concentrations of IL-10 and TGF-β in cell supernatants, as well as reduced IL-1β and TNF-α in RAW264.7 cells with sh-IRF9 compared to the control group. These results suggest that IRF9 is implicated in the regulation of macrophage polarization and secretion.

In the past few years, an increasing number of research investigations have indicated that IRF9 is involved in cell proliferation, tumor formation, inflammation, autoimmune diseases and immune cell regulation [30,31]. In a mouse model of colitis induced by sodium dextrose sulfate, it has been found that IRF9 forms a complex with STAT1, and thus the pro-inflammatory response generated by both plays a crucial part in the progression of colitis, whereas knockdown of IRF9 exerted a protective effect in mice [32]. In this investigation, sh-IRF9 RAW264.7 was observed to exhibit a beneficial impact on mice with CIA. Injection of sh-IRF9 RAW264.7 reduced the degree of arthritis. The expression of iNOS was decreased in the sh-IRF9 group compared to the CIA group, while CD206 was gradually increased. The distribution of macrophages was dominated by M2 type, M1/M2 ratio was regulated and sh-IRF9 RAW264.7 decreased the expression of pro-inflammatory factors and increased anti-inflammatory factors in the serum of mice. These results confirmed our speculation that IRF9 was associated with altered macrophage function.

In this research, the investigation of IRF9's involvement in RA was conducted for the first time, providing experimental evidence for understanding the mechanism by which IRF9 regulates macrophage function in RA. The findings suggested that IRF9-mediated metabolic abnormalities in M1/M2 cells played a role in the pathogenesis of RA, and knockdown of IRF9 in RAW264.7 cells alleviated arthritic inflammation in CIA mice. The potential mechanism involved the regulation of macrophage function by IRF9 through PSMA5, thereby contributing to the inflammatory immune response. Additional examination is required to elucidate the molecular mechanism underlying the role of IRF9 in modulating macrophage function.

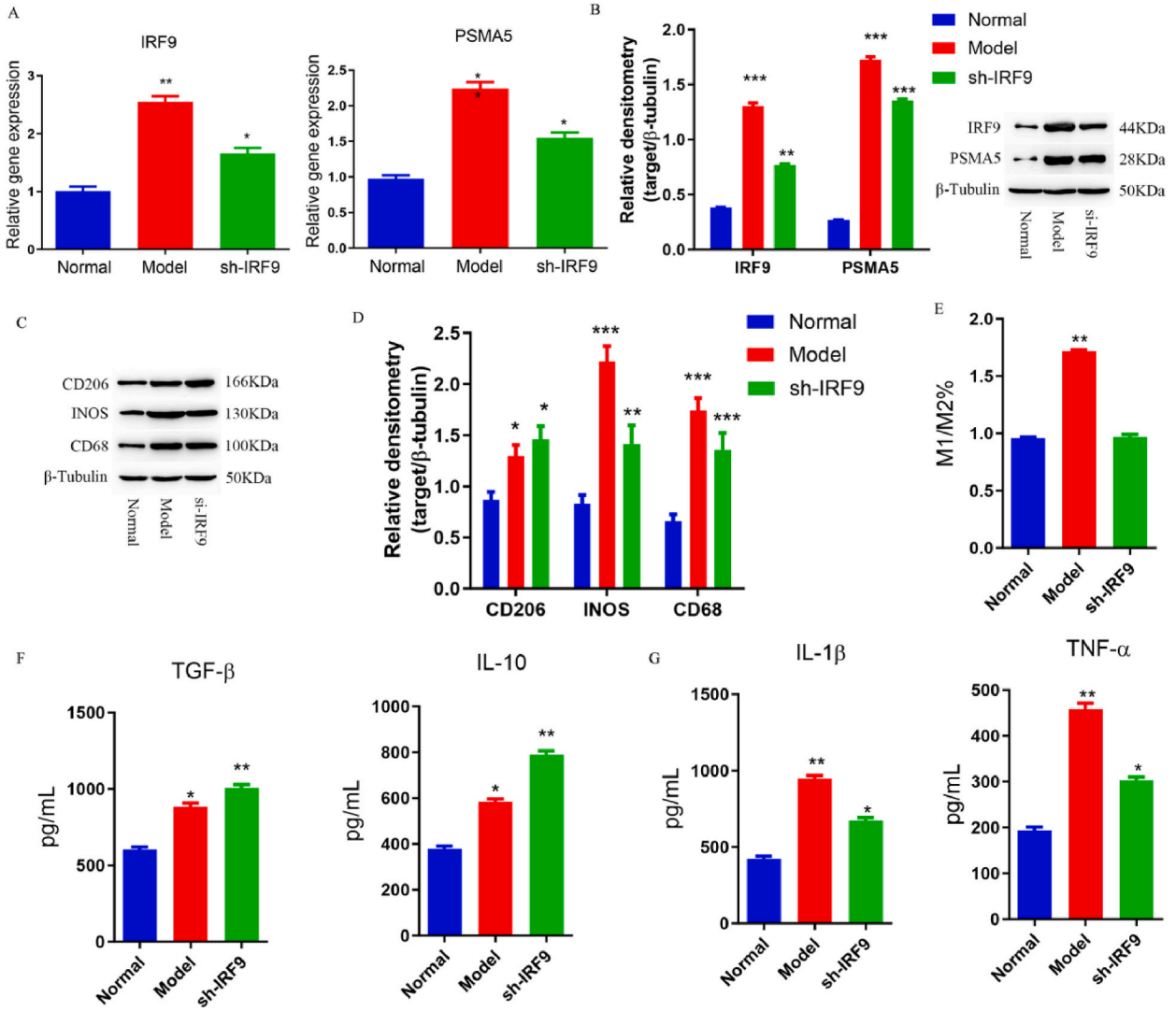

Fig. 6. IRF9 regulates macrophage M1/M2 polarization and switching in CIA mice. A-B. qRT-PCR and Western blot for the expression of IRF9 and PSMA5. C-D. Western blot for CD68, iNOS and CD206. E. Proportion of M1 and M2 type macrophages. F. ELISA for the expression of TGF-β and IL-10. G. ELISA for the expression of TNF-α and IL-1β. Data were expressed as mean ± standard deviation (n = 6), *p < 0.05.

5. Conclusion

There are fewer studies on the role played by IRF9 in the pathogenesis of RA, and no study has yet demonstrated IRF9 in RA through its involvement in the regulation of macrophage polarization. The present study utilized bioinformatic analysis and experimental validation to identify the overexpression of IRF9 in RA. Furthermore, a combination of in vitro and ex vivo experiments was conducted to elucidate the role and molecular mechanism of IRF9-mediated macrophage activation in immunometabolic disorders associated with RA. These findings provide valuable experimental evidence for the identification of novel drug targets aimed at treating RA.

Availability of data and materials

All experimental data included in this study can be obtained by contacting the first author if needed.

Ethics approval and consent to participate

The study was approved by the Ethics Committee of The Third Affiliated Hospital of Qiqihar Medical University(NO. 2023LL-69).

The animal experiment was approved by the Animal Ethical Care Committee of the Third Affiliate Hospital of Qiqihar Medical University (NO.AECC- 2023-003).

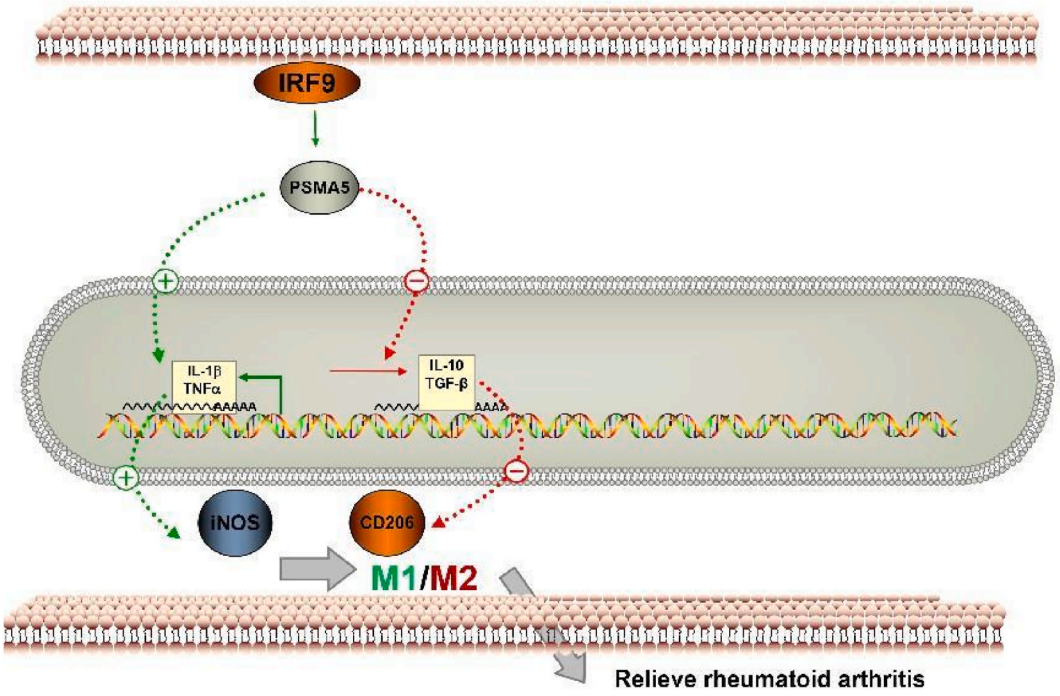

Fig. 7. IRF9 promotes pro-inflammatory factor TNF by increasing PSMA5 gene expression- α, IL-1 β Level, reduce anti-inflammatory factor TGF- β And IL-10 levels promote an increase in the proportion of M1/M2 cells, which are involved in the regulation of rheumatoid arthritis.

Funding

Funding for this study was provided by Funding for Basic Research Operating Expenses Project of Provincial Undergraduate Universities in Heilongjiang Province in 2023(2023-KYYWF-0878).

CRediT authorship contribution statement

Yue Guan: Writing – review & editing, Writing – original draft, Formal analysis, Conceptualization. **Xin Li:** Writing – review & editing, Project administration. **Hemin Yang:** Writing – review & editing, Resources. **Siyu Xu:** Writing – review & editing, Resources. **Lidong Shi:** Writing – review & editing, Data curation. **Yangyang Liu:** Writing – review & editing, Resources. **Lingdan Kong:** Writing – review & editing, Data curation. **Ying Qin:** Writing – review & editing, Writing – original draft, Formal analysis, Conceptualization.

Declaration of competing interest

The authors declare that they have no known competing financial interests or personal relationships that could have appeared to influence the work reported in this paper.

Acknowledgment

Not applicable.

Appendix A. Supplementary data

Supplementary data to this article can be found online at https://doi.org/10.1016/j.heliyon.2024.e35589.

References

[1] A.F. Radu, S.G. Bungau, Management of rheumatoid arthritis: an overview, Cells 10 (11) (2021 Oct 23) 2857, https://doi.org/10.3390/cells10112857. PMID: 34831081; PMCID: PMC8616326.

[2] H.U. Scherer, T. Häupl, G.R. Burmester, The etiology of rheumatoid arthritis, J. Autoimmun. 110 (2020 Jun) 102400, https://doi.org/10.1016/j.jaut.2019.102400. Epub 2020 Jan 22. PMID: 31980337.

[3] P. Prasad, S. Verma, Ganguly NK. Surbhi, V. Chaturvedi, S.A. Mittal, Rheumatoid arthritis: advances in treatment strategies, Mol. Cell. Biochem. 478 (1) (2023 Jan) 69–88, https://doi.org/10.1007/s11010-022-04492-3. Epub 2022 Jun 21. PMID: 35725992.

[4] K. Ishigaki, S. Sakaue, C. Terao, et al., Multi-ancestry genome-wide association analyses identify novel genetic mechanisms in rheumatoid arthritis, Nat. Genet. 54 (11) (2022) 1640–1651, https://doi.org/10.1038/s41588-022-01213-w.

[5] S. Smith, T. Fernando, P.W. Wu, et al., MicroRNA-302d targets IRF9 to regulate the IFN-induced gene expression in SLE, J. Autoimmun. 79 (2017) 105–111, https://doi.org/10.1016/j.jaut.2017.03.003.

[6] S. Han, H. Zhuang, P.Y. Lee, M. Li, L. Yang, P.A. Nigrovic, W.H. Reeves, Differential responsiveness of monocyte and macrophage subsets to interferon, Arthritis Rheumatol. 72 (1) (2020 Jan) 100–113, https://doi.org/10.1002/art.41072. Epub 2019 Dec 10. PMID: 31390156; PMCID: PMC6935410.

[7] J.W. Leavenworth, X. Lai, H. Miao, D. Wang, H. Zhao, Y. Li, Editorial: macrophage immunity and metabolism in cancer: novel diagnostic and therapeutic strategies, Front. Immunol. 13 (2022 Dec 16) 1113031, https://doi.org/10.3389/fimmu.2022.1113031. PMID: 36591256; PMCID: PMC9800978.

[8] M. Vierhout, A. Ayoub, S. Naiel, P. Yazdanshenas, S.D. Revill, A. Reihani, A. Dvorkin-Gheva, W. Shi, K. Ask, Monocyte and macrophage derived myofibroblasts: is it fate? A review of the current evidence, Wound Repair Regen. 29 (4) (2021 Jul) 548–562, https://doi.org/10.1111/wrr.12946. Epub 2021 Jun 9. PMID: 34107123.

[9] M. Cutolo, R. Campitiello, E. Gotelli, S. Soldano, The role of M1/M2 macrophage polarization in rheumatoid arthritis synovitis, Front. Immunol. 13 (2022 May 19) 867260, https://doi.org/10.3389/fimmu.2022.867260. PMID: 35663975; PMCID: PMC9161083.

[10] C. Yunna, H. Mengru, W. Lei, C. Weidong, Macrophage M1/M2 polarization, Eur. J. Pharmacol. 877 (2020 Jun 15) 173090, https://doi.org/10.1016/j.ejphar.2020.173090. Epub 2020 Mar 29. PMID: 32234529.

[11] A. Nawaz, M. Bilal, S. Fujisaka, et al., Depletion of CD206+ M2-like macrophages induces fibro-adipogenic progenitors activation and muscle regeneration, Nat. Commun. 13 (1) (2022) 7058, https://doi.org/10.1038/s41467-022-34191-y. Published 2022 Nov 21.

[12] A. Nawaz, M. Bilal, S. Fujisaka, et al., Depletion of CD206+ M2-like macrophages induces fibro-adipogenic progenitors activation and muscle regeneration, Nat. Commun. 13 (1) (2022) 7058, https://doi.org/10.1038/s41467-022-34191-y. Published 2022 Nov 21.

[13] Y. Yan, L. Zheng, Q. Du, et al., Interferon regulatory factor 1(IRF-1) activates anti-tumor immunity via CXCL10/CXCR3 axis in hepatocellular carcinoma (HCC), Cancer Lett. 506 (2021) 95–106, https://doi.org/10.1016/j.canlet.2021.03.002.

[14] J. Qiu, B. Xu, D. Ye, et al., Cancer cells resistant to immune checkpoint blockade acquire interferon-associated epigenetic memory to sustain T cell dysfunction, Nat. Can. (Ott.) 4 (1) (2023) 43–61, https://doi.org/10.1038/s43018-022-00490-y.

[15] M. Hu, Y. Zhang, X. Li, et al., TLR4-Associated IRF-7 and NFκB signaling act as a molecular link between androgen and metformin activities and cytokine synthesis in the PCOS endometrium, J. Clin. Endocrinol. Metab. 106 (4) (2021) 1022–1040, https://doi.org/10.1210/clinem/dgaa951.

[16] F. Jiang, H.Y. Zhou, L.F. Zhou, W. Zeng, L.H. Zhao, IRF9 affects the TNF-induced phenotype of rheumatoid-arthritis fibroblast-like synoviocytes via regulation of the SIRT-1/NF-κB signaling pathway, Cells Tissues Organs 209 (2–3) (2020) 110–119, https://doi.org/10.1159/000508405.

[17] M. Kloc, A. Subuddhi, A. Uosef, J.Z. Kubiak, R.M. Ghobrial, Monocyte-macrophage lineage cell fusion, Int. J. Mol. Sci. 23 (12) (2022) 6553, https://doi.org/10.3390/ijms23126553. Published 2022 Jun 12.

[18] J. Huang, X. Fu, X. Chen, Z. Li, Y. Huang, C. Liang, Promising therapeutic targets for treatment of rheumatoid arthritis, Front. Immunol. 12 (2021) 686155, https://doi.org/10.3389/fimmu.2021.686155. Published 2021 Jul 9.

[19] S. Alivernini, L. MacDonald, A. Elmesmari, et al., Distinct synovial tissue macrophage subsets regulate inflammation and remission in rheumatoid arthritis, Nat. Med. 26 (8) (2020) 1295–1306, https://doi.org/10.1038/s41591-020-0939-8.

[20] I. Pérez-Díez, Z. Andreu, M.R. Hidalgo, et al., A comprehensive transcriptional signature in pancreatic ductal adenocarcinoma reveals new insights into the immune and desmoplastic microenvironments, Cancers 15 (11) (2023) 2887, https://doi.org/10.3390/cancers15112887. Published 2023 May 24.

[21] H. Schmidt, P. Braubach, C. Schilpp, et al., IL-13 impairs tight junctions in airway epithelia, Int. J. Mol. Sci. 20 (13) (2019) 3222, https://doi.org/10.3390/ijms20133222. Published 2019 Jun 30.

[22] F. Lu, J. Zhou, Q. Chen, et al., PSMA5 contributes to progression of lung adenocarcinoma in association with the JAK/STAT pathway, Carcinogenesis 43 (7) (2022) 624–634, https://doi.org/10.1093/carcin/bgac046.

[23] Z. Fu, C. Lu, C. Zhang, B. Qiao, PSMA5 promotes the tumorigenic process of prostate cancer and is related to bortezomib resistance, Anti Cancer Drugs 30 (7) (2019) e0773, https://doi.org/10.1097/CAD.0000000000000773.

[24] Q. Li, F. Tan, Y. Wang, et al., The gamble between oncolytic virus therapy and IFN, Front. Immunol. 13 (2022) 971674, https://doi.org/10.3389/fimmu.2022.971674. Published 2022 Aug 25.

[25] W. Liu, S. Zhang, J. Wang, IFN-γ, should not be ignored in SLE, Front. Immunol. 13 (2022) 954706, https://doi.org/10.3389/fimmu.2022.954706. Published 2022 Aug 10.

[26] H. Negishi, T. Taniguchi, H. Yanai, The interferon (IFN) class of cytokines and the IFN regulatory factor (IRF) transcription factor family, Cold Spring Harbor Perspect. Biol. 10 (11) (2018) a028423, https://doi.org/10.1101/cshperspect.a028423. Published 2018 Nov 1.

[27] Q.T. Pham, N. Oue, Y. Sekino, et al., TDO2 overexpression is associated with cancer stem cells and poor prognosis in esophageal squamous cell carcinoma, Oncology 95 (5) (2018) 297–308, https://doi.org/10.1159/000490725.

[28] N. Kondo, T. Kuroda, D. Kobayashi, Cytokine networks in the pathogenesis of rheumatoid arthritis, Int. J. Mol. Sci. 22 (20) (2021) 10922, https://doi.org/10.3390/ijms222010922. Published 2021 Oct 10.

[29] N. Komatsu, H. Takayanagi, Mechanisms of joint destruction in rheumatoid arthritis - immune cell-fibroblast-bone interactions, Nat. Rev. Rheumatol. 18 (7) (2022) 415–429, https://doi.org/10.1038/s41584-022-00793-5.

[30] C.A. Jefferies, Regulating IRFs in IFN driven disease, Front. Immunol. 10 (2019) 325, https://doi.org/10.3389/fimmu.2019.00325. Published 2019 Mar 29.

[31] S. Mishra, V.K. Maurya, S. Kumar, Kaur A. Ankita, S.K. Saxena, Clinical management and therapeutic strategies for the thyroid-associated ophthalmopathy: current and future perspectives, Curr. Eye Res. 45 (11) (2020) 1325–1341, https://doi.org/10.1080/02713683.2020.1776331.

[32] I. Rauch, F. Rosebrock, E. Hainzl, et al., Noncanonical effects of IRF9 in intestinal inflammation: more than type I and type III interferons, Mol. Cell Biol. 35 (13) (2015) 2332–2343, https://doi.org/10.1128/MCB.01498-14.